

# Formation of interference patterns in diffuse fields at spatial filtering of the diffraction field of the double-exposure Fresnel hologram

V.G. Gusev

Tomsk State University

Received April 7, 2004

The holographic interferometer sensitivity to cross or longitudinal motions of a plane diffusing surface is analyzed. It is shown, that the interferometer sensitivity depends on radius of curvature of the spherical wave used for the surface illumination, and on its distance to the photographic plate at the stage of the hologram recording. The experimental results are in a good agreement with the theoretical predictions.

One of the problems solved with the help of static holographic interferometry and speckle interferometry, is the inverse problem. It should predict the shape of the interference fringes and the place of their localization for the known optical system geometry. With this purpose in the published works including, for example Refs. 1 to 5, the mechanism of formation of the holographic interference patterns, sensitive to the diffuser's motions in the diffuse fields, was described following the geometric optics or using the analysis of light diffraction on a set of reflective gratings. However, the indirect researches (for example, Refs. 6–8), connected with the cross motion of a plane diffusing surface have shown that the holographic interference patterns can localize in two planes. This circumstance points out that in the mechanism of formation of the interference patterns it is necessary to consider the objective speckles' properties in the hologram plane. Hence, it is necessary to uniquely determine the holographic interferometer sensitivity to a particular motion of a diffuse surface.

In this paper conditions and features of the interference patterns' formation are analyzed at the double-exposure recording of the Fresnel hologram with the purpose of determination of the interferometer sensitivity to cross or longitudinal motions of a plane diffusing surface.

According to Fig. 1, the matt screen 1 that is in the plane  $(x_1, y_1)$ , is illuminated with a coherent radiation of a diverging spherical wave with the radius of curvature  $R_1$ . The diffuse scattered radiation is recorded during the first exposure on a photographic plate 2, which is in the plane  $(x_2, y_2)$ , with the help of the off-axis plane reference wave. The quantity  $\theta$  is the angle that makes a reference beam with a normal to a photographic plate's plane. Before the re-exposure, the matt screen is moved in its plane, for example along the direction toward the  $x$ -axis by the distance  $a$ .

In the Fresnel approximation disregarding the constant factors, the distribution of the complex field

amplitude, corresponding to the first exposure, in the object channel in a photographic plate's plane is written as follows

$$u_1(x_2, y_2) \sim \iint_{-\infty}^{\infty} t(x_1, y_1) \exp\left[\frac{ik}{2R_1}(x_1^2 + y_1^2)\right] \times \exp\left\{\frac{ik}{2l_1}[(x_1 - x_2)^2 + (y_1 - y_2)^2]\right\} dx_1 dy_1, \quad (1)$$

where  $k$  is the wave number;  $l_1$  is the distance between the planes  $(x_1, y_1)$ , and  $(x_2, y_2)$ ;  $t(x_1, y_1)$  is the complex transmission amplitude of the matt screen, being a random function of the coordinates.

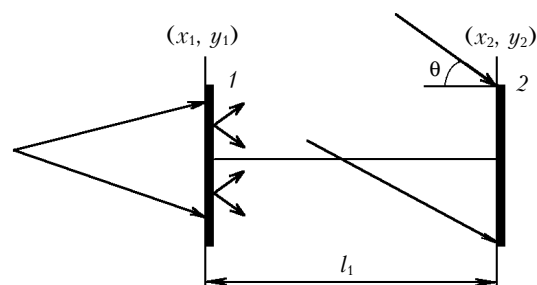


Fig. 1. Diagram of the Fresnel hologram recording: 1 is the matt screen; 2 is the photographic plate.

Let us present expression (1) in the following form:

$$u_1(x_2, y_2) \sim \exp\left[\frac{ik}{2l_1}(x_2^2 + y_2^2)\right] \times \left\{ F_1(x_2, y_2) \otimes \exp\left[-\frac{ikR_1}{2l_1(R_1 + l_1)}(x_2^2 + y_2^2)\right] \right\}, \quad (2)$$

where  $\otimes$  is the symbol of the convolution operation,  $F_1(x_2, y_2)$  is the Fourier image of the function  $t(x_1, y_1)$  with the spatial frequencies  $x_2/\lambda l_1$ , and  $y_2/\lambda l_1$ ,  $\lambda$  is the

wavelength of the coherent light used for recording and reconstruction of a hologram.

From Eq. (2) it follows that in the plane  $(x_2, y_2)$  the quasi-Fourier image of the matt screen's transmission function is formed, each point of which is widened to the size of the objective speckle<sup>9</sup> because of the spatial boundedness of the diffraction field, caused by finite sizes of the diffuser area illuminated. Thus on the objective speckles the phase distribution of the diverging spherical wave with the radius of curvature  $l_1$  is superposed.

Distribution of the complex field amplitude for the second exposure in an object channel in a photographic plate's plane

$$u_2(x_2, y_2) \sim \int_{-\infty}^{\infty} \int_{-\infty}^{\infty} t(x_1 + a, y_1) \exp\left[\frac{ik}{2R_1}(x_1^2 + y_1^2)\right] \times \exp\left\{\frac{ik}{2l_1}[(x_1 - x_2)^2 + (y_1 - y_2)^2]\right\} dx_1 dy_1 \quad (3)$$

takes, after Fourier transforms, the following form

$$u_2(x_2, y_2) \sim \exp\left(\frac{ikax_2}{l_1}\right) \exp\left[\frac{ik}{2l_1}(x_2^2 + y_2^2)\right] \times \left\{F_1(x_2, y_2) \otimes \exp\left[-\frac{ikR_1}{2l_1(R_1 + l_1)}(x_2^2 + y_2^2)\right] \times \exp\left(\frac{-ikax_2}{l_1}\right)\right\}. \quad (4)$$

On the basis of Eqs. (2) and (4) the complex transmission amplitude of the double-exposure hologram, corresponding to the  $(-1)$ st diffraction order, under condition of recording of the photographic plate blackening in the linear range is determined by the expression

$$\tau(x_2, y_2) \sim \exp(-ikx_2 \sin \theta) \left\{ \exp\left[\frac{ik}{2l_1}(x_2^2 + y_2^2)\right] \times \left\{F_1(x_2, y_2) \otimes \exp\left[-\frac{ikR_1}{2l_1(R_1 + l_1)}(x_2^2 + y_2^2)\right]\right\} + \exp(ikax_2/l_1) \exp\left[\frac{ik}{2l_1}(x_2^2 + y_2^2)\right] \left\{F_1(x_2, y_2) \otimes \exp\left[-\frac{ikR_1}{2l_1(R_1 + l_1)}(x_2^2 + y_2^2)\right] \exp\left(\frac{-ikax_2}{l_1}\right)\right\} \right\}. \quad (5)$$

Let at the stage of the hologram reconstruction a spatial filtering of the diffraction field is carried out in its plane and on the optical axis with the help of a round aperture in the opaque screen  $p$  (Fig. 2).

Thus within the limits of a filtering aperture's diameter, the phase changes are  $(kax_2/l_1) \leq \pi$ . Then distribution of the complex field amplitude at the output of a spatial filter takes the following form:

$$u(x_2, y_2) \sim p(x_2, y_2) \exp\left[\frac{ik}{2l_1}(x_2^2 + y_2^2)\right] \times \left\{ \left\{F_1(x_2, y_2) \otimes \exp\left[-\frac{ikR_1}{2l_1(R_1 + l_1)}(x_2^2 + y_2^2)\right]\right\} + \left\{F_1(x_2, y_2) \otimes \exp\left[-\frac{ikR_1}{2l_1(R_1 + l_1)}(x_2^2 + y_2^2)\right] \exp(-ikax_2/l_1)\right\} \right\}, \quad (6)$$

where  $p(x_2, y_2)$  is the transmission function of a spatial filter.<sup>10</sup>

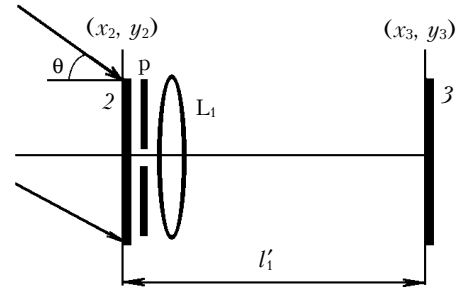


Fig. 2. Diagram of recording the interference pattern localized in a plane of the diffuser image formation: 2 is the hologram; 3 is the interferogram recording plane;  $L_1$  is the lens;  $p$  is the spatial filter.

Let's consider, that the positive lens  $L_1$  (Fig. 2) with a focal length  $f_1$  is in the hologram plane and the distance of  $l'_1$  satisfies the condition  $(1/l'_1) = (1/f) - (1/l_1)$ . Besides, here and further for reducing the length of formulas we shall consider, that  $l'_1 = l_1$ , and do not take into account the factors which are insignificant for the final result. Then distribution of the complex field amplitude in the plane  $(x_3, y_3)$  of the diffuser image formation is determined by the expression

$$u(x_3, y_3) \sim t(-x_3, -y_3) \exp\left[\frac{ik(R_1 + l_1)}{2l_1 R_1}(x_3^2 + y_3^2)\right] \times \left\{1 + \exp\left[\frac{ik(R_1 + l_1)ax_3}{l_1 R_1}\right]\right\} \otimes P(x_3, y_3), \quad (7)$$

where  $P(x_3, y_3)$  is the Fourier image of the function  $p(x_2, y_2)$  with the spatial frequencies  $x_3/\lambda l_1$ , and  $y_3/\lambda l_1$ .

If in Eq. (7) the period of functional change  $1 + \exp[ik(R_1 + l_1)ax_3/l_1 R_1]$  is at least one order longer,<sup>11</sup> than the  $P(x_3, y_3)$  function width, which determines the size of the subjective speckle in the plane  $(x_3, y_3)$ , we shall remove it from the convolution integral symbol. Then distribution of the illumination over the recording plane 3 (Fig. 2) takes the following form

$$I(x_3, y_3) \sim [1 + \cos(kG_1 ax_3/l_1)] |t(-x_3, -y_3)| \times \exp\left[\frac{ik(R_1 + l_1)}{2l_1 R_1}(x_3^2 + y_3^2)\right] \otimes P(x_3, y_3)^2, \quad (8)$$

where  $G_1 = (R_1 + l_1)/R_1$  is the coefficient introduced to characterize the change of the interferometer sensitivity depending on  $R_1$  and  $l_1$ .

From Eq. (8) it follows that within the limits of diffuser image the subjective speckle-structure is modulated by the interference fringes, which periodically alternate in the direction of its motion, and measurement of period of the interference fringes provides an opportunity to determine  $a$ .

Let now, at the stage of the hologram reconstruction, a spatial filtering of the diffraction field be carried out on the optical axis in the plane  $(x_3, y_3)$  (Fig. 3) of the diffusing plane image.

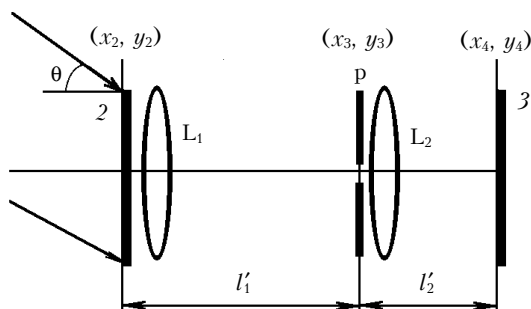


**Fig. 3.** Diagram of recording the interference pattern localized in the hologram plane: 2 is the hologram; 3 is the interferogram recording plane;  $L_1$  and  $L_2$  are the lenses; p is the spatial filter.

In this case, ignoring the spatial boundedness of the field because of the hologram finite size (or of the lens  $L_1$ ), the distribution of the complex field amplitude at the exit of a spatial filter, if the phase change within the filtering aperture,  $(kG_1ax_3/l_1) \leq \pi$ , is described by the expression

$$\begin{aligned}
 u(x_3, y_3) \sim & p(x_3, y_3) \exp\left[\frac{ik}{2l_1}(x_3^2 + y_3^2)\right] \times \\
 & \times \left\{ t(-x_3, -y_3) \exp\left[\frac{ik(R_1 + l_1)}{2R_1l_1}(x_3^2 + y_3^2)\right] + \right. \\
 & \left. + t(-x_3, -y_3) \exp\left[\frac{ik(R_1 + l_1)}{2R_1l_1}(x_3^2 + y_3^2)\right] \otimes \right. \\
 & \left. \otimes \exp\left[-\frac{ik}{2l_1}[(x_3 - a)^2 + y_3^2]\right] \otimes \exp\left[\frac{ik}{2l_1}(x_3^2 + y_3^2)\right] \right\}. \quad (9)
 \end{aligned}$$

Assume that the positive lens  $L_2$  (Fig. 3) with a focal length of  $f_2$  is in a spatial filter's plane. Besides, here and below we shall consider, for the sake of brevity, that  $l'_2 = l'_1 = l_1$  and  $f_2 = l_1/2$ . Then the distribution of the complex field amplitude in the plane  $(x_4, y_4)$  of the hologram image formation takes the form

$$\begin{aligned}
 u(x_4, y_4) \sim & \left\{ F_1(-x_4, -y_4) \otimes \exp\left[-\frac{ikR_1}{2l_1(R_1 + l_1)}(x_4^2 + y_4^2)\right] \right\} \times \\
 & \times [1 + \exp(-ikax_4/l_1)] \otimes P(x_4, y_4), \quad (10)
 \end{aligned}$$

where  $P(x_4, y_4)$  is the Fourier image of the function  $p(x_3, y_3)$  with the spatial frequencies  $x_4/\lambda l_1$  and  $y_4/\lambda l_1$ .

On the basis of Eq. (10) distribution of illumination over the plane 3 (Fig. 3) when the period of functional change  $1 + \exp(-ikax_4/l_1)$  exceeds the  $P(x_4, y_4)$  function width, which characterizes the size of the subjective speckle in the plane  $(x_4, y_4)$ , is determined, allowing for the sign of a tilt angles of the wave fronts, by the following expression

$$\begin{aligned}
 I(x_4, y_4) \sim & [1 - \cos(kax_4/l_1)] |F_1(-x_4, -y_4) \otimes \\
 & \otimes \exp\left[-\frac{ikR_1}{2l_1(R_1 + l_1)}(x_4^2 + y_4^2)\right] \otimes P(x_4, y_4)|^2. \quad (11)
 \end{aligned}$$

It is necessary to mention, that in deriving the expressions (8) to (11) the constant phase component  $k(R_1 + l_1)a^2/2R_1l_1$  was not taken into account because of its smallness.

From Eq. (11) it follows, that in the hologram plane the periodic, along the direction of the diffuser motion, interference fringes modulate the subjective speckle-structure. Thus, the interferometer sensitivity to cross motion does not depend on radius of curvature  $R_1$  of a diverging spherical wave used for illumination of the matt screen 1 (see Fig. 1).

The localization of the interference patterns in two planes: in the hologram plane and in the plane of formation of the image of a plane diffusing surface, is caused by that, on the one hand, the objective speckles in the hologram plane contain the information on the phase distribution of a diverging spherical wave with the radius of curvature  $l_1$ . On the other hand, in the hologram plane there is a displacement of the objective speckles corresponding to the second exposure by the identical distance. It is explained by that for the light field scattered by the matt screen 1 (see Fig. 1), every spatial frequency participating in the formation of the objective speckle, corresponding to the second exposure, is displaced by the same distance compared with the spectrum, which corresponds to the first exposure. Besides for the fixed values  $a$  and  $l_1$  the displacement of the objective speckles increases with the decrease of the radius of curvature  $R_1$  of a diverging wave front, used for the diffuser's illumination. For this reason, the interferometer sensitivity (Fig. 4) to cross motion increases if the interference pattern is recorded in the plane of formation of the image of the diffusing surface, where the identical speckles of two exposures are combined when performing a spatial filtering of the diffraction field in the hologram plane.

At the stage of the double-exposure hologram's recording, the matt screen 1 (see Fig. 1) is illuminated with a coherent radiation of a converging spherical wave. Therefore, the interference fringes' frequency in the interference pattern localized in the hologram plane as well as in the case of the diffuser illumination by radiation of a diverging spherical wave also does not depend on radius of curvature  $R_1$ . However, in recording the interference pattern localized in the plane of the

diffuser image formation, the interferometer sensitivity changes by  $G_2 = (R_1 - l_1)/R_1$  times. In this case, the interferometer sensitivity decreases down to zero, as it follows from Fig. 4 at a fixed  $l_1$ , as the radius of curvature decreases from  $R_1 = \infty$  down to  $R_1 = l_1$ .

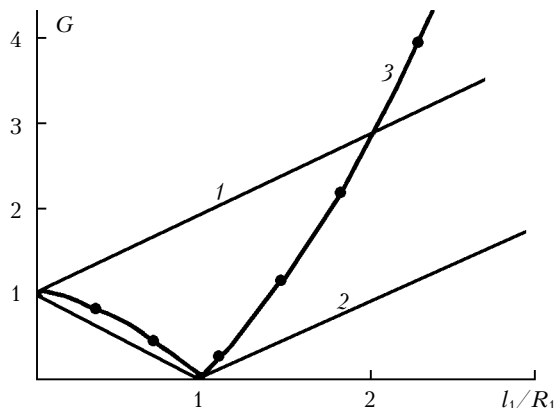


Fig. 4. Dependences of the interferometer sensitivity coefficients on the radius of curvature of a spherical wave front for  $l_1 = 250$  mm:  $G_1$  (1);  $G_2$  (2);  $G_3$  (3).

This circumstance is connected with the reduction of the displacement of the objective speckles corresponding to the second exposure in the hologram plane. Moreover, at  $R_1 = l_1$  the identical objective speckles of two-exposures coincide in the hologram plane except only for a tilt angle between the speckle-fields of two-exposures determined by the ratio  $a/l_1$ . As a result, the interference pattern is localized only in the hologram plane ("frozen" interference fringes). It is typical of the interference pattern that it does not change at variation of the observation angle if there is a positive lens with the focal length  $f \leq l_1$  in the hologram plane. Further reduction of the radius of curvature  $R_1$  leads to the displacement of the identical objective speckles corresponding to the second exposure. This displacement leads to the interferometer sensitivity increase (see Fig. 4) at recording the interference pattern localized in a plane of the diffuser image formation.

Let the matt screen 1 (see Fig. 1) be displaced, before a photographic plate re-exposure, along the  $z$ -axis by the distance of  $\Delta l = l_2 - l_1$ , and  $\Delta l \ll l_1$ . Then, allowing for the constant phase factors, distribution of the complex transmission amplitude of the double-exposure hologram, corresponding to the  $(-1)$ st order of diffraction, in the Fresnel approximation takes the following form

$$\begin{aligned} \tau'(x_2, y_2) \sim \exp(-ikx_2 \sin \theta) & \left\{ \exp(ikl_1) \exp \left[ \frac{ik}{2l_1} (x_2^2 + y_2^2) \right] \times \right. \\ & \times \left\{ F_1(x_2, y_2) \otimes \exp \left[ -\frac{ikR_1}{2l_1(R_1 + l_1)} (x_2^2 + y_2^2) \right] \right\} + \\ & \left. + \exp(ikl_2) \exp \left[ \frac{ik}{2l_2} (x_2^2 + y_2^2) \right] \right\} F_1(x_2, y_2) \otimes \end{aligned}$$

$$\otimes \exp \left[ -\frac{ikR_2 l_2}{2l_1^2(R_2 + l_2)} (x_2^2 + y_2^2) \right] \Bigg\}, \quad (12)$$

where  $R_2 = R_1 - \Delta l$ .

If at the stage of the hologram reconstruction spatial filtering is carried out of the diffraction field (see Fig. 2) in the hologram plane on the optical axis, and the phase change  $[k\Delta l - k\Delta l(x_2^2 + y_2^2)/2l_2^2] \leq \pi$ , within the limits of a filtering aperture's diameter the distribution of the complex field amplitude over the plane of the diffuser image formation is determined by the expression

$$\begin{aligned} u'(x_3, y_3) \sim t(-x_3, -y_3) \exp \left[ \frac{ik(R_1 + l_1)}{2R_1 l_1} (x_3^2 + y_3^2) \right] \times \\ \times \left\{ 1 + \exp \left[ -\frac{ik(R_1^2 - l_1^2)\Delta l}{2R_1^2 l_1^2} (x_3^2 + y_3^2) \right] \right\} \otimes P(x_3, y_3). \quad (13) \end{aligned}$$

When in Eq. (13) the function variation period  $1 + \exp \left[ -\frac{ik(R_1^2 - l_1^2)\Delta l}{2R_1^2 l_1^2} (x_3^2 + y_3^2) \right]$  is longer, than the  $P(x_3, y_3)$  function width, distribution of illumination over the plane of recording 3 (see Fig. 2) takes the form

$$\begin{aligned} I'(x_3, y_3) \sim \left\{ 1 + \cos \left[ \frac{kG_3 \Delta l}{2l_1^2} (x_3^2 + y_3^2) \right] \right\} \left\{ t(-x_3, -y_3) \times \right. \\ \left. \times \exp \left[ \frac{ik(R_1 + l_1)}{2R_1 l_1} (x_3^2 + y_3^2) \right] \otimes P(x_3, y_3) \right\}^2, \quad (14) \end{aligned}$$

where  $G_3 = (R_1^2 - l_1^2)/R_1^2$  is the coefficient introduced to characterize the interferometer sensitivity variation depending on the  $R_1$  and  $l_1$  quantities.

From Eq. (14) it follows, that within the limits of the diffuser image, the fringes of an equal tilt (the system of concentric rings) modulate the subjective speckle-structure and measurement of the rings' radii in the next orders of interference, enables one to determine  $\Delta l$  value.

Let spatial filtering of the diffraction field be performed at the stage of the hologram reconstruction on an optical axis in the  $(x_3, y_3)$  plane (see Fig. 3) of the diffuser image formation. In this case distribution of the complex field amplitude over the plane  $(x_4, y_4)$  of the hologram image formation, if the phase change  $[kG_3 \Delta l(x_3^2 + y_3^2)/2l_1^2] \leq \pi$  within the limits of a filtering aperture, is determined by the following expression

$$\begin{aligned} u'(x_4, y_4) \sim \left\{ F_1(-x_4, -y_4) \otimes \exp \left[ -\frac{ikR_1}{2l_1(R_1 + l_1)} (x_4^2 + y_4^2) \right] \right\} \times \\ \times \left\{ 1 + \exp \left\{ i \left[ k\Delta l - \frac{k\Delta l}{2l_1^2} (x_4^2 + y_4^2) \right] \right\} \right\} \otimes P(x_4, y_4). \quad (15) \end{aligned}$$

From Eq. (15) it follows that the distribution of illumination in the plane 3 (see Fig. 3), assuming that the function period  $1 + \exp\{i[k\Delta l - k\Delta l(x_4^2 + y_4^2)/2l_1^2]\}$  exceeds the  $P(x_4, y_4)$  function width, takes the following form

$$I(x_4, y_4) \sim \left\{ 1 + \cos \left[ k\Delta l - \frac{k\Delta l}{2l_1^2}(x_4^2 + y_4^2) \right] \right\} |F_1(-x_4, -y_4) \otimes \exp \left[ -\frac{ikR_1}{2l_1(R_1 + l_1)}(x_4^2 + y_4^2) \right] \otimes P(x_4, y_4)|^2. \quad (16)$$

According to the expression (16) in the plane of the hologram image formation, the interference pattern in the form of the rings modulates the subjective speckle structure. Thus, the interferometer sensitivity to the diffuser longitudinal motion does not depend on the radius of curvature  $R_1$  of the diverging spherical wave used for the matt screen 1 illumination (see Fig. 1). Besides, as in the case of interference patterns' formation, when before the re-exposure the diffuser is moved across, the opposite phase change along the interference pattern's coordinate occurs compared to that in the interference pattern localized in the plane of the diffuser image formation.

If at the stage of the double-exposure hologram's recording the matt screen 1 (see Fig. 1) is illuminated with a coherent radiation of a converging spherical wave, then taking into account that  $R_2 = R_1 + \Delta l$ , the interference rings' radii in the interference pattern localized in the hologram plane, also do not depend on  $R_1$ . Thus, for the interference pattern localized in the plane of the diffuser image formation, the interferometer sensitivity to longitudinal motion of the plane diffuse surface also changes by  $G_3$  times.

In the considered case of the interference patterns' formation, the objective speckles in the hologram plane bear information on the phase distribution of the diverging spherical waves with the radii of curvature  $l_1$  and  $l_2$  as it follows from the expression (12). This circumstance, on the one hand, provides the interference patterns' localization in the hologram plane and independence of the interference rings' radii in it of  $R_1$ . On the other hand, in the general case identical objective speckles of two exposures within the limits of small area of the photographic plate on the optical axis coincide in the hologram plane. In spite of this, the objective speckles, corresponding to the second exposure, have the tilt angle changing along the radius from the optical axis. Besides at a fixed  $l_1$  the tilt angle decreases with the decrease of  $|R_1|$  within the limits of  $l_1 \leq |R_1| \leq \infty$  that leads to the sensitivity reduction down to zero (see Fig. 4) to the diffuser longitudinal motion for the interference pattern localized in the plane of its image formation.

Further reduction of the radius of curvature when  $|R_1| \leq l_1$ , is accompanied by the tilt angle increase of the identical speckles, corresponding to

the second exposure that leads to an increase of the interferometer sensitivity at recording of the interference pattern localized in the plane of the diffuser image formation. Within a rather narrow interval of  $|R_1|$  values in the vicinity of  $|R_1| = l_1$ , which satisfies the condition

$$|kG_3\Delta l(D/2)^2/2l_1^2| \leq \pi,$$

where  $D$  is the illuminated area diameter of the matt screen 1 (see Fig. 1), in the hologram plane only a spatial separation of the objective speckles of second and first exposures occurs along the radius from the optical axis.

Consequently, at  $|R_1| = l_1$  the recording of the interference pattern localized in the hologram plane needs for spatial filtering of the diffraction field to be performed on the optical axis in the plane of the diffuser image formation, although no interference pattern corresponding to the expression (14) is observed in this plane.

To prove this, we shall limit ourselves to consideration of the case of the matt screen illumination 1 (see Fig. 1) with the radiation of a converging spherical wave with radius of curvature  $R_1 = l_1$ . Then the distribution of the complex transmission amplitude of the double-exposure hologram, corresponding to the  $(-1)$ st order of diffraction, takes the form

$$\tau(x_2, y_2) \sim \exp(-ikx_2 \sin \theta) \left\{ \exp(ikl_1) \exp \left[ \frac{ik}{2l_1}(x_2^2 + y_2^2) \right] \times \right. \\ \left. \times F_1(x_2, y_2) + \exp(ikl_2) \exp \left[ \frac{ik}{2l_2}(x_2^2 + y_2^2) \right] F_2(x_2, y_2) \right\}, \quad (17)$$

where  $F_2(x_2, y_2)$  is the Fourier image of the function  $t(x_1, y_1)$  with the spatial frequencies  $x_2/\lambda l_2$ , and  $y_2/\lambda l_2$ .

At the hologram reconstruction (see Fig. 3) the distribution of the complex field amplitude in the plane  $(x_3, y_3)$  of the diffuser image formation, at the exit of a spatial filter, is determined by the expression

$$u'(x_3, y_3) \sim p(x_3, y_3) \exp \left[ \frac{ik}{2l_1}(x_3^2 + y_3^2) \right] \times \\ \times \left\{ \exp(ikl_1)t(-x_3, -y_3) + \exp(ikl_2) \exp \left[ -\frac{ik}{2\Delta l}(x_3^2 + y_3^2) \right] \otimes \right. \\ \left. \otimes t \left( -\frac{l_2}{l_1}x_3, -\frac{l_2}{l_1}y_3 \right) \right\}. \quad (18)$$

If the diameter  $d$  of a filtering aperture satisfies the condition  $d \leq 2\lambda l_1^2/D\Delta l$ , then in Eq. (18) it is possible to assume, that within the limits of a filtering aperture there are identical objective speckles of two exposures, i.e.

$$t(-x_3, -y_3) = t \left( -\frac{l_2}{l_1}x_3, -\frac{l_2}{l_1}y_3 \right).$$

Then distribution of the complex field amplitude in the plane  $(x_4, y_4)$  of the hologram image formation takes the following form

$$u'(x_4, y_4) \sim \left\{ 1 + \exp \left[ i \left[ k\Delta l + \frac{k\Delta l}{2l_1^2} (x_4^2 + y_4^2) \right] \right] \right\} \times \\ \times F_1(-x_4, -y_4) \otimes P(x_4, y_4), \quad (19)$$

and the distribution of illumination in it, is determined by the expression

$$I'(x_4, y_4) \sim \left\{ 1 + \cos \left[ k\Delta l + \frac{k\Delta l}{2l_1^2} (x_4^2 + y_4^2) \right] \right\} \times \\ \times |F_1(-x_4, -y_4) \otimes P(x_4, y_4)|^2. \quad (20)$$

In its turn, when performing a spatial filtering of the diffraction field in the hologram plane at a point, for example, with the coordinates  $x_{02}, 0$  distribution of the complex field amplitude at the exit of a spatial filter takes the form

$$u'(x_2, y_2) \sim p(x_2, y_2) \times \\ \times \left\{ \exp(ikl_1) \times \exp \left[ \frac{ik}{2l_1} [(x_2 + x_{02})^2 + y_2^2] \right] \right\} \times \\ \times F_1(x_2 + x_{02}, y_2) + \exp(ikl_2) \times \\ \times \exp \left[ \frac{ik}{2l_2} [(x_2 + x_{02})^2 + y_2^2] \right] F_2(x_2 + x_{02}, y_2). \quad (21)$$

When the positive lens  $L_1$  constructs (see Fig. 2) the diffuser image in the plane  $(x_3, y_3)$  and the phase change of the interference pattern localized in the hologram plane does not exceed  $\pi$ , the distribution of the complex field amplitude in it, within the limits of a filtering aperture, is determined by the expression

$$u'(x_3, y_3) \sim \left\{ \exp \left[ \frac{ik}{l_1} x_{02} (x_3 - x_{02}) \right] t(-x_3 + x_{02}, -y_3) + \right. \\ \left. + \exp \left[ \frac{ik}{l_1} \left( 1 - \frac{\Delta l}{l_1} \right) x_{02} (x_3 - x_{02}) \right] \right\} \times \\ \times t \left[ -\frac{l_2}{l_1} (x_3 - x_{02}), -\frac{l_2}{l_1} y_3 \right] \otimes P(x_3, y_3). \quad (22)$$

If a filtering aperture's diameter satisfies the condition  $d \leq 2\lambda l_1^2 / D\Delta l$ , then, disregarding the phase constant value, distribution of illumination over the plane  $(x_3, y_3)$  takes the following form

$$I'(x_3, y_3) \sim \left[ 1 + \cos(kx_{02}\Delta l x_3 / l_1^2) \right] \times \\ \times \left| \exp(ikx_{02}x_3 / l_1) t(-x_3 + x_{02}, -y_3) \otimes P(x_3, y_3) \right|^2. \quad (23)$$

From Eq. (23) it follows that the subjective speckle-structure is modulated by the equidistant along the  $x$ -axis interference fringes. Thus, the

interference fringes' frequency increases with the distance from the optical axis where spatial filtering of the diffraction field is being done that is caused by the increase of the displacement in the hologram plane along a radius from the optical axis of the objective speckles, corresponding to the second exposure, relative to their position at the first exposure. Besides it is necessary to note, that in a plane of the diffuser image formation, as well as in the all above-stated cases, the interference pattern's localization is provided due to the conservation of information on the phase distribution of a diverging spherical wave by the objective speckles.

In experiment the double-exposure Fresnel holograms were recorded on the photographic plates of a Mikrat-VRL type with the radiation of a He-Ne laser at the wavelength of  $0.63 \mu\text{m}$ . The technique of experiment consists in comparison of the results of the hologram recording for the fixed values of both the cross  $a = (0.025 \pm 0.002) \text{ mm}$ , and longitudinal motion  $\Delta l = (1.85 \pm 0.002) \text{ mm}$ . Thus, the distance between the matt screen and a photographic plate  $l_1$  was 250 mm, and the various radii of curvature of the diverging or converging spherical waves were selected within the limits from  $R_1 = \infty$  up to  $|R_1| = 125 \text{ mm}$ . The diameter of the illuminated area of the matt screen was about 30 mm.

As an example in Fig. 5 the interference patterns localized in the plane of the diffuser image formation and characterizing its cross motion are presented.

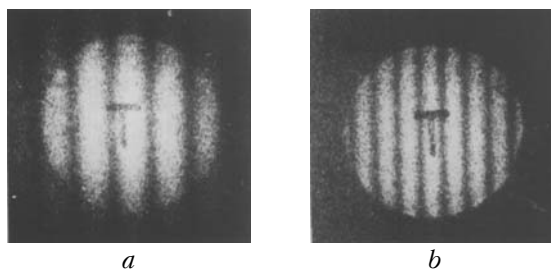


**Fig. 5.** The interference patterns localized in the plane of the diffuser image formation and characterizing its cross motion: for  $R_1 = \infty$  (a); for  $R_1 = 350 \text{ mm}$  (b).

The "T" mark has been preliminary drawn on the matt screen. The interference patterns were recorded at spatial filtering of the diffraction field in the hologram plane by reconstructing it with a small-diameter ( $\approx 2 \text{ mm}$ ) laser beam. Figure 5a corresponds to the matt screen 1 illumination (see Fig. 1) by a collimated beam and Fig. 5b to a diverging spherical wave with the radius of curvature  $R_1 = 350 \text{ mm}$ . In these cases, as well as in the subsequent one, with the change of both the magnitude and the sign of  $R_1$ , the interference patterns localized in the hologram plane, had the identical frequency of the interference fringes, corresponding to the fringe frequency in Fig. 5a. A spatial filtering of the diffraction field in a plane of the diffuser image formation (see Fig. 3) was carried out with a filtering aperture of 2-mm diameter.

By measuring periods of the interference fringes, the coefficients  $G_1$  and  $G_2$  were determined (besides,

the coefficients  $G$  can be determined from the measured values of  $l_1$  and  $R_1$ ). The values of  $G_1$  and  $G_2$  obtained in that way corresponded to Fig. 4 accurate to 10%, admitted in the experiment, and to results of the indirect researches in Refs. 6 to 8, that used the diffuser cross motion.

The interference patterns in Fig. 6 are localized in the plane of the diffuser image formation and characterize its longitudinal motion, when at the double-exposure hologram recording the matt screen 1 (see Fig. 1) was illuminated with a collimated beam.

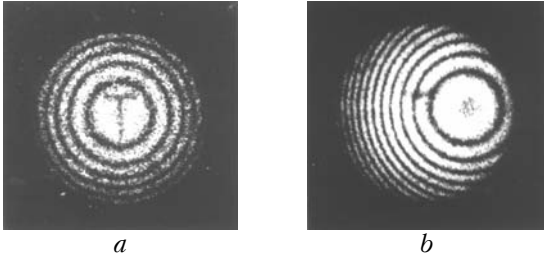


**Fig. 6.** The interference patterns localized in a plane of the diffuser image formation, characterizing its longitudinal motion and corresponding to realization of a spatial filtering of the diffraction field on the optical axis (*a*) and out of the optical axis (*b*).

Their recording was carried out similarly to recording of the interference patterns characterizing the diffuser cross motion. Thus, Fig. 6*a* corresponds to the spatial filtering of the diffraction field on the optical axis, Fig. 6*b* shows the case of filtering made at a distance of  $x_{02} = 9$  mm from it. In the last case, distribution of the complex field amplitude in the  $(x_2, y_2)$  hologram plane (see Fig. 2) takes the following form

$$\begin{aligned}
 u'(x_2, y_2) \sim & p(x_2, y_2) \left\{ \exp(ikl_1) \times \right. \\
 & \times \exp\left\{ \frac{ik}{2l_1} [(x_2 + x_{02})^2 + y_2^2] \right\} \left. \left\{ F_1(x_2 + x_{02}, y_2) \otimes \right. \right. \\
 & \otimes \exp\left\{ -\frac{ik}{2l_1} [(x_2 + x_{02})^2 + y_2^2] \right\} \right\} + \\
 & + \exp(ikl_2) \exp\left\{ \frac{ik}{2l_2} [(x_2 + x_{02})^2 + y_2^2] \right\} \times \\
 & \times \left\{ F_1(x_2 + x_{02}, y_2) \otimes \exp\left\{ -\frac{ik}{2l_2} [(x_2 + x_{02})^2 + y_2^2] \right\} \right\}. \quad (24)
 \end{aligned}$$

If the phase change of the interference pattern localized in the hologram plane does not exceed  $\pi$ , within the limits of the filtering aperture, the distribution of the complex field amplitude in the  $(x_3, y_3)$  plane (see Fig. 2) of the diffuser image formation, without the account of a constant phase component  $k\Delta l$ , is determined by the following expression

$$u'(x_3, y_3) \sim t(-x_3 + x_{02}, -y_3) \exp\left\{ \frac{ik}{2l_1} [(x_3 + x_{02})^2 + y_3^2] \right\} \times$$

$$\times \left\{ 1 + \exp\left[ -\frac{ik\Delta l}{2l_1^2} (x_3^2 + y_3^2) \right] \right\} \otimes P(x_3, y_3), \quad (25)$$

according to which, the distribution of illumination over this plane takes the form

$$\begin{aligned}
 I'(x_3, y_3) \sim & \left\{ 1 + \cos\left[ \frac{k\Delta l}{2l_1^2} (x_3^2 + y_3^2) \right] \right\} \times \\
 & \times |t(-x_3 + x_{02}, -y_3) \exp\left\{ \frac{ik}{2l_1} [(x_3 + x_{02})^2 + y_3^2] \right\} \otimes \\
 & \otimes P(x_3, y_3)|^2. \quad (26)
 \end{aligned}$$

As follows from Eq. (26), the center of the plane diffusing surface shifts, at the  $x_{02}$  change, relative to the position of the interference pattern's center that is caused by the parallax phenomenon. Besides, the change of  $x_{02}$  results in the interference pattern's phase change from 0 up to  $\pi$ , when the center of a filtering aperture moves in the interference pattern localized in the hologram plane from the interference fringe's minimum to its maximum, ("live" interference fringes). The same dynamics of the interference patterns' behavior takes place also in the case of reconstruction of the double-exposure Fresnel hologram, the recording of which was carried out for determination of the size of the diffuser cross motion.

The interference patterns in Fig. 7 are localized in the plane of the diffuser image formation and characterize its longitudinal motion. At the stage of the hologram recording, the matt screen 1 (see Fig. 1) was illuminated with a diverging spherical wave with  $R_1 = 350$  mm (Fig. 7*a*) or with a converging spherical wave with  $R_1 = 125$  mm (Fig. 7*b*).

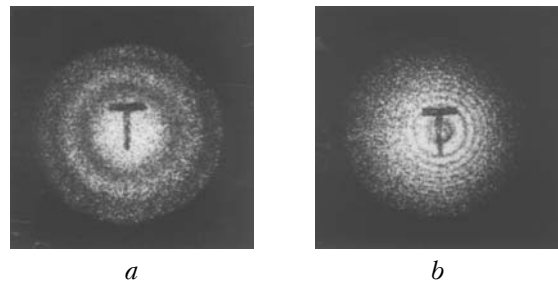


**Fig. 7.** The interference patterns localized in the plane of the diffuser image formation characterizing its longitudinal motion:  $R_1 = 350$  mm (*a*);  $R_1 = 125$  mm (*b*).

In Figs. 6*a* and 7 the coefficient  $G_3$  values determined from measured radii of interference rings in the adjacent orders of interference, correspond to those in Fig. 4. Thus in all cases, connected with the change of  $R_1$  magnitude and sign, the number of interference fringes in the interference pattern localized in the hologram plane keeps the same within the limits of the collimated beam's diameter (equal to 30 mm) used to reconstruct it.

At illumination of the matt screen 1 (see Fig. 1) by a converging spherical wave with  $R_1 = l_1$ , the

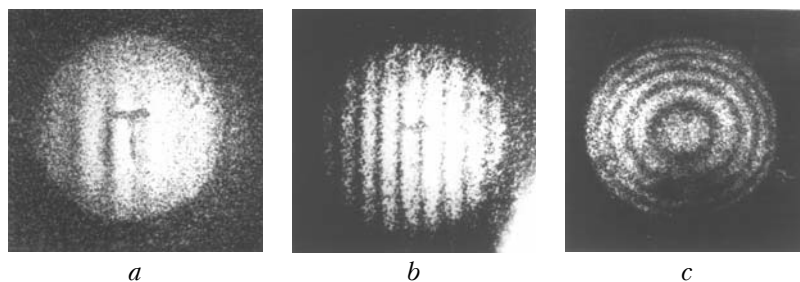


**Fig. 8.** The interference patterns localized in the plane of the diffuser image formation (*a*, *b*) and in the hologram plane (*c*), which characterize longitudinal motion of the diffuser when  $|R_1| = l_1$ .

interference patterns are localized in the plane of the diffuser image formation (Figs. 8*a* and *b*). And their recording was carried out using filtering in the hologram plane aperture of 0.7 mm diameter at displacement of its center relative to the optical axis by  $x_{02} = 4.3$  (Fig. 8*a*) and 7.8 mm (Fig. 8*b*). Thus, the periods of the interference fringes correspond to the expression (23).

In its turn, the realization of a spatial filtering of the diffraction field on the optical axis in the plane of the diffuser image formation (see Fig. 3) with a filtering aperture of 0.7 mm diameter is accompanied by the interference pattern's formation localized in the hologram plane (Fig. 8*c*). For it, the interference rings' radii in the adjacent orders of interference satisfy the expression (20). The double-exposure Fresnel hologram possesses similar properties, when the matt screen *1* (see Fig. 1) is illuminated with a diverging spherical wave with  $R_1 = l_1$ .

It is necessary to note, that accomplishment of the double-exposure hologram recording, the lensless quasi-Fourier-hologram, does not lead to the change of *G* coefficients. The difference was that the diffuser and the interference pattern's images in its plane were formed in far diffraction zone. Besides, when performing a spatial filtering of the diffraction field in the hologram's plane out of the optical axis, the interference pattern shifts relative to the motionless diffuser in the plane of its image formation.

In the case of the diffuser illumination with a converging spherical wave with  $R_1 = l_1$  (lensless Fourier hologram), the "frozen" interference pattern, localized in the hologram plane and characterizing the cross motion, is observed without the use of a positive lens because no phase distribution of a diverging spherical wave exists in the hologram plane.

Thus, the study performed has shown the following.

In the general case of the double-exposure Fresnel hologram recording the interference patterns

characterizing both cross and longitudinal motion of a plane diffusing surface are localized in two planes: in the plane of the diffuser image formation and in the hologram plane. It is worthy to note that the change of the phase of the interference patterns with the varying coordinate is opposite in them. Sensitivity to the interference pattern's motions localized in the hologram plane depends on the distance between the diffuser and the photographic plate at the stage of the hologram recording.

Sensitivity of the interference pattern localized in the plane of the diffuser image formation to its cross motion depends, in addition to the above-mentioned distance, on the radius of curvature of the spherical wave used for illumination of the diffuser and on its sign. At the same time the interference pattern's sensitivity characterizing the longitudinal motion of the plane diffusing surface localized in the plane of its image formation, does not depend on the sign of the radius of curvature of the spherical wave used to illuminate the diffusing screen.

## References

1. N.E. Molin and K.A. Stetson, *Optik* **31**, No. 3, 157–177 (1970).
2. D.A. Gregory, *Opt. Acta* **27**, No. 4, 481–510 (1980).
3. I. Prikril, *Opt. Application* **10**, No. 1, 3–11 (1980).
4. M. Yonemura, *Opt. Acta* **27**, No. 11, 1537–1549 (1980).
5. R.D. Bahuguna, S.C. Lee, and N.H. Abramson, *Proc. Soc. Photo-Opt. Instrum. Eng.* **954**, 50–57 (1989).
6. V.G. Gusev, *Atmos. Oceanic Opt.* **12**, No. 8, 645–650 (1999).
7. V.G. Gusev, *Vestn. Tomsk State Univ.*, No. 278, Ser. Fiz., 87–94 (2003).
8. V.G. Gusev, *Vestn. Tomsk State Univ.*, No. 278, Ser. Fiz., 95–103 (2003).
9. M. Franson, *Speckle Optics* [Russian translation] (Mir, Moscow, 1980), 158 pp.
10. M. Born and E. Wolf, *Principles of Optics* (Pergamon Press, Oxford–London–New York, 1964).